Microscopic theory for charge transports of ruthenate

Naoya ARAKAWA
Department of Physics, The University of Tokyo
Bunkyo-ku, Hongo, Tokyo 113-0033

In strongly correlated electron systems near a magnetic quantum-critical point (QCP), many-body effect of electron correlation causes unusual transport properties (TPs) deviating from the Fermi liquid (FL). One of the examples is cuprate: near an antiferromagnetic (AF) QCP, the in-plane resistivity, ρ_{ab}, and Hall coefficient, $R_{\rm H}$, show the T-linear dependence and Curie-Weiss (CW) like T dependence, respectively. Another is ruthenate near an AF or a ferromagnetic QCP: in $Sr_2Ru_{0.075}Ti_{0.025}O_4$, near the AF QCP, ρ_{ab} shows the T-linear dependence; in $Ca_{2-x}Sr_xRuO_4$ around $x = 0.5$, near the FM QCP, ρ_{ab} and $R_{\rm H}$ show the $T^{1.4}$ dependence and CW like T dependence, respectively. Note that ρ_{ab} and $R_{\rm H}$ show the FL behaviors.

For cuprate, the origins of these non-FL behaviors in ρ_{ab} and $R_{\rm H}$ have been clarified by fluctuation-exchange (FLEX) approximation with Maki-Thompson (MT) current vertex correction (CVC), the correction of the current due to MT electron-hole (el-h) four-point vertex function (VF). The T-linear ρ_{ab} arises from the strong T and $\boldsymbol{k}$ dependence of the quasiparticle (QP) damping; the CW like T dependence of $R_{\rm H}$ arises from the strong T and $\boldsymbol{k}$ dependence of MT el-h four-point VF; these dependence of the QP damping and MT el-h four-point VF arise from the CW like T dependence of the spin susceptibility at $\boldsymbol{k} = (\pi, \pi)$.

Although the roles of the QP damping and MT el-h four-point VF will be significant in multiorbital systems, these roles have not been clarified yet due to a large numerical cost arising from the large mesh of the Brillouin zone and the number of the Matsubara frequencies.

In this project, to clarify the roles of the QP damping and the MT el-h four-point VF in the charge transports of ruthenate, I analyze ρ_{ab} and $R_{\rm H}$ for the t_{2g} orbital Hubbard model on a square lattice by the FLEX approximation with the MT CVC [1]; ρ_{ab} and $R_{\rm H}$ (in the weak-field limit) are formulated by using the Kubo formula and considering the most divergent terms with respect to the QP lifetime. Technically, I resolve the numerical difficulty about the large numerical cost explained above by constructing an optimized algorithm, where without using a rotational symmetry, the memory and time of the calculations are about eight times smaller than those for a usual algorithm.

I have revealed the roles and achieved qualitative agreement with experiments. The main contribution arises from the $d_{xz/yz}$ orbital due to the smaller QP damping and larger band velocity of that orbital than those of the d_{xy} orbital. Also, the non-FL like QP damping of the $d_{xz/yz}$ orbital near the AF QCP causes the T-linear ρ_{ab}. Moreover, the MT CVC arising from the non-diagonal spin fluctuation at $\boldsymbol{k} = (0.66\pi, 0.66\pi)$ between the $d_{xz/yz}$ and d_{xy} orbitals causes the negative enhancement and the peak at low T as a result of the sign change and enhancement of the component of the transverse conductivity of the d_{xy} orbital.

References

[1] N. Arakawa, Ph. D. Thesis, The University of Tokyo (2014); in preparation.

Origin of the correlation between the Fermi surface shape and T_c in the cuprate superconductors

KAZUHIKO KUROKI
Department of Physics, Osaka University
1-1 Machikaneyama, Toyonaka, Osaka, 560-0043, Japan

CORRELATION BETWEEN THE FERMI SURFACE SHAPE AND T_c

In 2001, Pavarini *et al.* showed for the cuprate superconductors that there is a correlation between the experimentally observed T_c and the Fermi surface warping[1]. Namely, they have obtained single-orbital tight-binding models for various cuprates to estimate the ratio "r" between the nearest and second-neighbor hoppings, which is a measure of the warping of the Fermi surface. Plotting the experimental T_c against the theoretically evaluated r, they showed that T_c systematically increases with the Fermi surface warping.

In an attempt to investigate the origin of this correlation, we have previously introduced a two-orbital model that explicitly considers the d_{z^2} Wannier orbital on top of the $d_{x^2-y^2}$[2, 3]. There, we showed that ΔE, the level offset between $d_{x^2-y^2}$ and d_{z^2} orbitals, dominates both of the warping of the Fermi surface and T_c. It was shown that La_2CuO_4, despite its less warped (more nested) Fermi surface, has lower T_c than those of $HgBa_2CuO_4$, $Tl_2Ba_2CuO_6$, and $Bi_2Sr_2CuO_6$ due to a strong d_{z^2} orbital mixture on the Fermi surface that degrades T_c. However, among the above mentioned four single-layer cuprates, only La_2CuO_4 has a small ΔE (i.e., a strong d_{z^2} mixture), so that we are still in need of a convincing study as to whether ΔE is systematically controlling T_c in a wider range of cuprates, including the multi-layered ones that were included in Pavarini's plot[1]. Hence, in the present project, we have examined the systematics by extending the analysis to bilayer cuprates as well as those single-layer ones that have relatively lower T_c [4].

MODEL CONSTRUCTION

First-principles electronic structures of the materials are obtained with the VASP package[5], where experimentally determined lattice parameters are adopted. We then employ the $d_{x^2-y^2}$ and d_{z^2} Wannier orbitals as projection functions[6] to model the band structure around the Fermi level. The calculation is performed for single-layer La_2CuO_4, $Pb_2Sr_2Cu_2O_6$, and bilayer $La_2CaCu_2O_6$, $Pb_2Sr_2YCu_3O_8$, $EuSr_2NbCu_2O_8$, $YBa_2Cu_3O_{7-\delta}$(YBCO), $HgBa_2CaCu_2O_6$(HBCO) and $Tl_2Ba_2CaCu_2O_8$. Experimentally, the first five materials are known to have relatively lower T_c's (below 70K), while the last three have higher T_c's (above 90K)[7].

We also construct *single*-orbital models for the above materials so that the main bands intersecting the Fermi level are reproduced with a single Wannier orbital per site. This Wannier orbital mainly consists of the $d_{x^2-y^2}$ orbital, but also has tails with a d_{z^2} orbital character. We can then define the parameter, $r = (|t_2| + |t_3|)/|t_1|$ in terms of the second (t_2) and third (t_3) neighbor hoppings of the single-orbital model, which is a direct measure of the Fermi surface warping[1]. For bilayer materials, r can be defined with hoppings within each layer. Since these materials have two sites per unit cell, with outer and inner Fermi surfaces, so that we can alternatively obtain the respective measures of the warping of the outer and inner Fermi surfaces as $r_{\rm outer,inner} = (|t_2 \pm t_{2\perp}| + |t_3 \pm t_{3\perp}|)/|t_1 \pm t_{1\perp}|$, where $t_{i\perp}$ is the interlayer hopping to the sites vertically above (or below) the i-th neighbor.

FLUCTUATION EXCHANGE ANALYSIS

In the the two-orbital model we consider intra- and inter-orbital electron-electron interactions. The intra-orbital U is considered to be in the range of 7-10t (where $t \simeq 0.45$ eV is the nearest-neighbor hopping) for the cuprates, so we take the intra-orbital $U = 3.0$ eV. The Hund's coupling J and the pair-hopping J' are typically $\sim 0.1U$, so we take $J = J' = 0.3$ eV. Here we observe the orbital rotational symmetry which gives the inter-orbital $U' = U - 2J = 2.4$ eV. We apply FLEX[8] to this multi-orbital Hubbard model, and solve the linearized Eliashberg equation. Its eigenvalue λ increases upon lowering the temperature, and reaches unity at $T = T_c$. Therefore λ at a fixed temperature can be used as a qualitative measure for T_c. The temperature is fixed at $k_{\rm B}T = 0.01$eV in the present calculation. The total band filling (number of electrons /site) is fixed at $n = 2.85$, for which the filling of the main band amounts to 0.85 (15 % hole doping). We take a $32 \times 32 \times 4$ k-point meshes for the three-dimensional lattice with 1024 Matsubara frequencies.

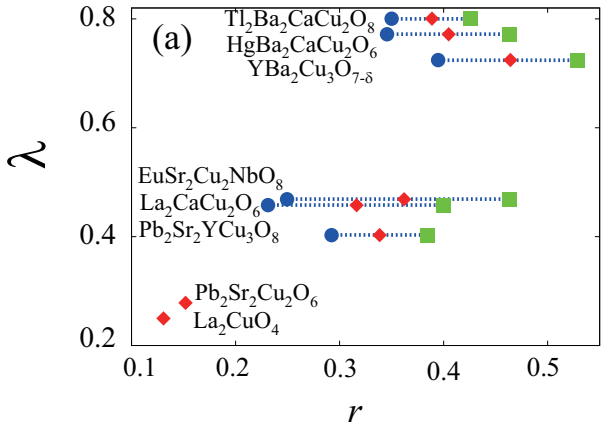

FIG. 1. Eigenvalue of the Eliashberg equation λ obtained for the two-orbital model plotted against r. $r_{\rm inner}$ and $r_{\rm outer}$ are also shown.

In Fig.1, we plot λ (obtained for the two-orbital model) against the measure of the Fermi surface warping r (of the single orbital model). The figure strikingly resembles Pavarini's plot[1] for the experimentally observed T_c against r. This resemblance unambigously shows that the T_c of the cuprates is strongly affected by the d_{z^2} orbital component mixture.

CONCLUSION

To conclude, constructing two- and single-orbital models of various bilayer as well as single-layer cuprates, we have revealed a systematic correlation between the Fermi surface warping and the theoretically evaluated T_c. Its striking resemblance with Pavarini's plot for experimental T_c's[1] unambiguously indicates that the d_{z^2} mixture is indeed a key factor that determines the T_c in the cuprates.

[1] E. Pavarini *et al.*, Phys. Rev. Lett. **87**, 047003 (2001).
[2] H. Sakakibara *et al.*, Phys. Rev. Lett. **105**, 057003 (2010).
[3] H. Sakakibara *et al.*, Phys. Rev. B **85**, 064501 (2012).
[4] H. Sakakibara *et al.*, arXiv : 1403.2497.
[5] G. Kresse and J. Hafner, Phys. Rev. B **47**, 558 (1993); G. Kresse and J. Furthmüller, Phys. Rev. B **54**, 11169 (1996) [http://cms.mpi.univie.ac.at/vasp/vasp/vasp.html]. Here we adopt GGA-PBEsol exchange correlation functional introduced by J. P. Perdew, A. Ruzsinszky, G. I. Csonka, O. A. Vydrov, G. E. Scuseria, L. A. Constantin, X. Zhou, and K. Burke, Phys. Rev. Lett. **100**, 136406 (2008), and the wave functions are expanded with plane waves up to a cut-off energy of 550 eV. 10^3 k-point meshes are used.
[6] N. Marzari and D. Vanderbilt, Phys. Rev. B **56**, 12847 (1997); I. Souza, N. Marzari and D. Vanderbilt, Phys. Rev. B **65**, 035109 (2001). The Wannier functions are generated by the code developed by A. A. Mostofi, J. R. Yates, N. Marzari, I. Souza and D. Vanderbilt, (http://www.wannier.org/).
[7] H. Eisaki *et al.*, Phys. Rev. B **69**, 064512 (2004).
[8] N.E. Bickers, D.J. Scalapino, and S.R. White, Phys. Rev. Lett. **62**, 961 (1989).

Stability of the superfluid state in three components fermionic optical lattices

AKIHISA KOGA
Department of Physics, Tokyo Institute of Technology
Meguro, Tokyo 152-8551, Japan

Ultracold atomic systems provide a variety of interesting topics. One of the active topics is the superfluid (SF) state in ultracold fermions, where interesting phenomena have been observed such as pseudogap behavior and the BCS-BEC crossover. Recently, degenerate multi-component fermionic systems have experimentally been realized,[1, 2, 3] which stimulates further theoretical investigation on the SF state in multi-component fermionic systems.

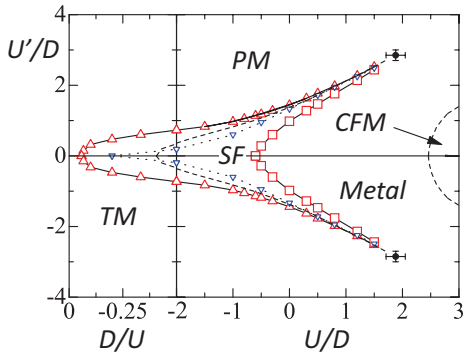

Figure 1: Phase diagram of the system at $T/D = 0.015$. Triangles (squares) represent the phase transition points between the SF and PM (metallic) states. The dashed lines represent the phase boundaries in the paramagnetic system. Dotted lines indicate the ridges of the pair potential in the SF state.

Motivated by this, we have studied low temperature properties of the three-component Hubbard model. By combining dynamical mean-field theory with a continuous-time quantum Monte Carlo method, we have obtained the finite temperature phase diagram, as shown in Fig. 1. We have found that the s-wave superfluid state proposed recently [4] is indeed stabilized in the repulsively interacting case and appears along the first-order phase boundary between the metallic and paired Mott states in the paramagnetic system [5]. Moreover, we have studied low-temperature properties in the BCS and BEC regions. It is found that the BCS state is characterized by the second-order phase transition, while the BEC state is by the first-order one. This is contrast to the two-component system, where the second-order phase transitions occur in both limits. It is also interesting how the SF state is realized in the multi-component fermionic systems for lithium and ytterbium atoms, which is now under consideration.

References

[1] T. B. Ottenstein et al., Phys. Rev. Lett. **101** 203202 (2008).

[2] T. Fukuhara et al., Phys. Rev. Lett. **98**, 030401 (2007).

[3] B. J. DeSalvo et al., Phys. Rev. Lett. **105**, 030402 (2010).

[4] K. Inaba and S. Suga, Phys. Rev. Lett. **108**, 255301 (2012); K. Inaba and S. Suga, Mod. Phys. Lett B **27** 1330008 (2013).

[5] Y. Okanami, N. Takemori and A. Koga: arXiv:1401.5610.

Numerical study of topological order

Y. Hatsugai
Division of Physics
Faculty of Pure and Applied Sciences, University of Tsukuba
1-1-1 Tennodai, Tsukuba 305-8571, Ibaraki, Japan

Numerical studies have been quite successful to describe phases of matter by evaluating correlation functions of local order parameters such as magnetization and pairing amplitudes of superconductors. Recent development of condensed matter physics motivates characterization of quantum phases from different aspects. One of such examples is an anisotropic superconductor where there can be a lot of phases even though all phases are supplemented by the gauge symmetry breaking as superconductivity. It clearly shows that the symmetry breaking is important but not enough. Then structure of the gap nodes of the superconductivity distinguishes the phases which is reflected by boundary states as the Andreev bound states. This is one of the typical examples of the bulk-edge correspondence which was discovered in the study of the quantum Hall effects. Today one may consider non trivial topological phases by the existence of the edges state governed by the bulk-edge correspondence. Then by using this bulk-edge correspondence, we define the topological order. In this sense, the edge states are kinds of order parameters. Then numerical studies are again quite important to directly observe these edge states. Also note that non trivial edge sates implies existence of non trivial Berry connections which characterizes the bulk.

Historical and very well known edge state is a dangling bond of the semiconductors. One may say that the edge states of graphene at the zigzag boundary belongs to this class. To use a symmetry breaking for the characterization of the phases, one needs to treat thermodynamic large systems. Contrary to this, topological order also works for a finite system. In this sense, we investigate topological properties of finite size graphene flakes by using Berry phases. As shown in Fig.1, existence of the dimers along the boundaries of some graphene flakes is clearly described by the Z_2 Berry phases[1].

We have also published several papers using the computer facilities at ISSP. Let us make a list of short descriptions for these works. Ref.[2,3]: calculation of the excitation gap is performed for the spin-resolve chiral condensate state of graphene under a strong magnetic field where many body interaction plays a crucial role. Ref.[4,5,6]: effects of chiral symmetry and randomness are studied numerically for multilayer graphene. Ref.[7-9]: bulk-edge correspondence is studied for massless/massive Dirac fermions.

References

[1] D. Seki, Y. Hamamoto and Y. Hatsugai, JPS Conf. Proc. 1, 012068 (2014)

Figure 1: An example of the Z_2 Berry phases for a graphene flake[1]. The red lines correspond to the links with the Berry phase π which implies there is a localized dimer on the link. The other blue links implies the Berry phases of the links are zero.

[2] Y. Hamamoto, T. Kawarabayashi, H. Aoki and Y. Hatsugai, Phys. Rev. B 88, 195141 (2013)

[3] Y.Hamamoto, H. Aoki, T. Kawarabayashi and Y. Hatsugai, J. Phys. Conf. Ser. 456, 012013 (2013)

[4] H. Sakamoto, Y. Hatsugai, H. Aoki and T. Kawarabayashi, JPS Conf. Proc. 1, 012069 (2014)

[5] T. Kawarabayashi, T. Honda, H. Aoki and Yasuhiro Hatsugai, AIP Conf. Proc. 1566, 283 (2013)

[6] T. Kawarabayashi, Y. Hatsugai and H. Aoki, J. Phys. Conf. Ser. 456, 012020 (2103)

[7] T. Kariyado and Y. Hatsugai, JPS Conf. Proc. 1, 012001 (2014)

[8] T. Kariyado and Y. Hatsugai, Phys. Rev. B 88, 245126 (2013)

[9] T. Fukui, K.-I. Imura and Y. Hatsugai, Journal of the Physical Society of Japan 82, 073708 (2013)

Numerical Study of Triangular Hubbard Models

Takami TOHYAMA*
Yukawa Institute for Theoretical Physics, Kyoto University
Kyoto 606-8502

Remarkable observations of a possible spin liquid phase and a new universality class of the metal-insulator transition in organic charge transfer salts have increased interest in these materials. It has been argued that a proper microscopic description of these materials can be given with a Hubbard model on the anisotropic triangular lattice at half filling. Parameters of the model for the description of organic charge transfer salts fall into the regime of strong correlations and significant frustration of antiferromagnetic spin interactions.

In this project, we have investigated two-magnon Raman scattering for organic charge transfer salts in collaboration with an experimental group [1]. Starting with an anisotropic triangular Hubbard model with 1st- and 2nd-neighbour hoppings and on-site Coulomb interaction, we set up an effective spin Hamiltonian after a strong-coupling expansion involving all possible processes up to the fourth order of the hopping terms. The resulting spin Hamiltonian contains all of the 1st-, 2nd-, and 3rd-neighbor exchange interactions together with four-spin ring-type exchange interactions. Performing exact-diagonalization calculations of two-magnon Raman scattering spectrum for a 27-site lattice, we have found that the polarization and material dependence of the spectrum are consistent with experimental data, suggesting a crucial role of frustration in these materials and a possible ground state of spin liquid.

We have also investigated the ground state property of a triangular Hubbard model with isotropic hoppings by density-matrix renormalization group (DMRG). In the ISSP supercomputer, we have performed small-scale calculations, while large scale calculations have been done on K Computer in Kobe. We note that the package of DMRG code for two-dimensional spin and Hubbard systems has been developed and is now available on several platforms including ISSP supercomputer and K computers. We calculated ground-state energy, double occupation number, entangle entropy, and spin-spin correlation function for cylindrical shape of the triangular Hubbard model as well as periodical systems with small system size. A signature of a metal-insulator transition and spin-liquid to order transition has been obtained.

These works were done in collaboration with Y. Nakamura, H. Kishida, S. Sota and J. Kokalj.

参考文献

[1] Y. Nakamura, N. Yoneyama, T. Sasaki, T. Tohyama, A. Nakamura, and H. Kishida: J. Phys. Soc. Jpn. in press.

*Present Address: Department of Applied Physics, Tokyo University of Science, Tokyo 125-8585

Research for Superconductivity in Strongly Correlated Multi-Orbital Systems

Yuji SHIBA and Takashi HOTTA
Department of Physics, Tokyo Metropolitan University
1-1 Minami-Osawa, Hachioji, Tokyo 192-0397

In this research, the effect of the Fermi-surface topology on the emergence of superconductivity is discussed in the two-dimensional $e_{\rm g}$-electron system coupled with Jahn-Teller phonons on the basis of the strong-coupling theory [1]. It is well known that the van Hove singularity occurs in the density of states due to the abrupt change of the Fermi-surface structure, leading to the enhancement of $T_{\rm c}$. We find that $T_{\rm c}$ is increased for the hopping parameters apart from the van Hove singularity point, when the $e_{\rm g}$-electron system possesses disconnected Fermi surfaces in comparison with the case of single Fermi surface. The increase of $T_{\rm c}$ is due to the large pair-hopping amplitude between different Fermi surfaces enhanced by the Jahn-Teller phonons.

We consider the two-dimensional square lattice and the lattice constant is taken as unity. The model Hamiltonian used here is given by

$$H = \sum_{\boldsymbol{k},\sigma,\gamma,\gamma'} \varepsilon_{\boldsymbol{k}\gamma\gamma'} d^{\dagger}_{\boldsymbol{k}\gamma\sigma} d_{\boldsymbol{k}\gamma'\sigma} + \sum_{\boldsymbol{q}} [g_2 \phi_{2\boldsymbol{q}} (\rho^{ab}_{\boldsymbol{q}} + \rho^{ba}_{\boldsymbol{q}}) + g_3 \phi_{3\boldsymbol{q}} (\rho^{aa}_{\boldsymbol{q}} - \rho^{bb}_{\boldsymbol{q}})] + \sum_{\boldsymbol{q}} (\omega_2 a^{\dagger}_{2\boldsymbol{q}} a_{2\boldsymbol{q}} + \omega_3 a^{\dagger}_{3\boldsymbol{q}} a_{3\boldsymbol{q}}), \quad (1)$$

where $d_{\boldsymbol{k}\gamma\sigma}$ denotes an annihilation operator of an $e_{\rm g}$ electron with spin σ and momentum $\boldsymbol{k}$ in the orbital γ (=a and b), a and b indicate x^2-y^2 and $3z^2-r^2$ orbitals, respectively, $\varepsilon_{\boldsymbol{k}aa} = (1/2)[3(dd\sigma) + (dd\delta)](\cos k_x + \cos k_y)$, $\varepsilon_{\boldsymbol{k}bb} = (1/2)[(dd\sigma) + 3(dd\delta)](\cos k_x + \cos k_y)$, $\varepsilon_{\boldsymbol{k}ab} = \varepsilon_{\boldsymbol{k}ab} = -(\sqrt{3}/2)[(dd\sigma) - (dd\delta)](\cos k_x - \cos k_y)$, $(dd\sigma)$ and $(dd\delta)$ denote the Slater-Koster integrals, $a_{2\boldsymbol{q}}$ and $a_{3\boldsymbol{q}}$ are annihilation operators for (x^2-y^2)- and $(3z^2-r^2)$-type Jahn-Teller phonons, respectively, g_2 and g_3 indicate electron-phonon coupling constants, $\phi_{2\boldsymbol{q}} = a_{2\boldsymbol{q}} + a^{\dagger}_{2-\boldsymbol{q}}$, $\phi_{3\boldsymbol{q}} = a_{3\boldsymbol{q}} + a^{\dagger}_{3-\boldsymbol{q}}$, $\rho^{\gamma\gamma'}_{\boldsymbol{q}} = \sum_{\boldsymbol{k},\sigma} d^{\dagger}_{\boldsymbol{k}+\boldsymbol{q}\gamma\sigma} d_{\boldsymbol{k}\gamma'\sigma}$, and ω_2 and ω_3 denote, respectively, Jahn-Teller phonon energies for (x^2-y^2)- and $(3z^2-r^2)$-type modes.

In order to calculate the superconducting transition temperature $T_{\rm c}$, we solve the linearlized gap equation obtained by evaluating both normal and anomalous electron self-energies due to the electron-phonon interaction. Here we consider the spin-singlet s-wave Cooper pair with the even function of frequency. In the second-order perturbation theory in terms of g_2 and g_3, the linearized gap equation at $T = T_{\rm c}$ is given by $\phi_{\mu\nu}(i\omega_n) = -T\sum_{n'}\sum_{\boldsymbol{k}}\sum_{\mu',\nu',\mu'',\nu''} V_{\mu\mu',\nu\nu'}(i\omega_n - i\omega_{n'}) G_{\mu'\mu''}(\boldsymbol{k}, i\omega_{n'}) G_{\nu'\nu''}(-\boldsymbol{k}, -i\omega_{n'}) \phi_{\mu''\nu''}(i\omega_{n'})$, where $\phi_{\mu\nu}(i\omega_n)$ is anomalous self-energy, $\omega_n = (2n+1)\pi T$ with a temperature T and an integer of n, G indicates the normal Green's function, given by $[G(\boldsymbol{k}, i\omega_n)]^{-1}_{\mu\nu} = [G^{(0)}(\boldsymbol{k}, i\omega_n)]^{-1}_{\mu\nu} - \Sigma_{\mu\nu}(i\omega_n)$, $G^{(0)}$ denotes the non-interacting electron Green's function, given by $[G^{(0)}]^{-1}_{\mu\nu} = (i\omega_n + \mu)\delta_{\mu\nu} - \varepsilon_{\boldsymbol{k}\mu\nu}$, μ is a chemical potential determined from the relation of $n = 2T\sum_n \sum_{\boldsymbol{k}} {\rm Tr} G(\boldsymbol{k}, i\omega_n)$, n is electron number per site, $\Sigma_{\mu\nu}(i\omega_n)$ denotes the normal electron self-energy, given by $\Sigma_{\mu\nu}(i\omega_n) = -T\sum_{n'}\sum_{\boldsymbol{k}'}\sum_{\mu',\nu'} V_{\mu\mu',\nu'\nu}(i\omega_n - i\omega_{n'}) G^{(0)}_{\mu'\nu'}(\boldsymbol{k}', i\omega_{n'})$. The phonon-mediated interaction $V_{\mu\mu',\nu\nu'}(i\nu_n)$ with $\nu_n = 2\pi T n$ is given

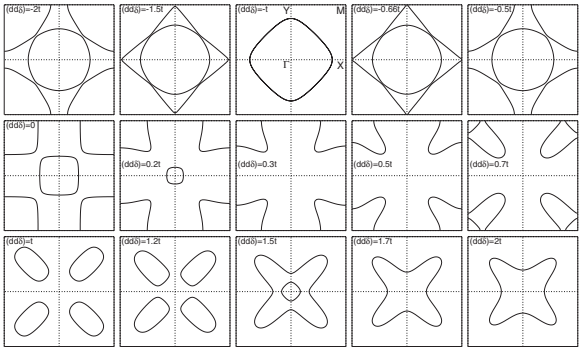

Figure 1: Variation of the Fermi surfaces for $(dd\sigma)/t = -1.0$ depicted in the first Brillouin zone of $-\pi \le k_x \le \pi$ and $-\pi \le k_y \le \pi$ with $\Gamma = (0,0)$, X=$(\pi,0)$, Y=$(0,\pi)$, and M=(π,π).

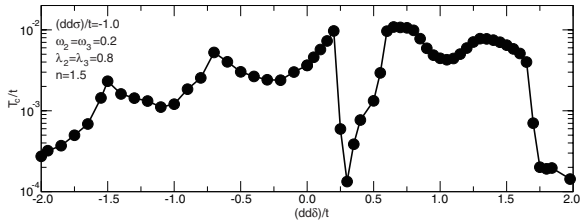

Figure 2: Superconducting transition temperature T_c/t vs. $(dd\delta)/t$ for $(dd\sigma)/t = -1.0$, $\omega_2/t = \omega_3/t = 0.2$, $\lambda_2 = \lambda_3 = 0.8$, and $n = 1.5$ in the range of $-2.0 \le (dd\delta)/t \le 2.0$.

by $V_{aa,aa} = V_{bb,bb} = -V_{aa,bb} = -V_{bb,aa} = g_3^2 D_3$, and $V_{ab,ab} = V_{ab,ba} = V_{ba,ab} = V_{ba,ba} = g_2^2 D_2$, where phonon Green's functions are given by $D_2 = 2\omega_2/[(i\nu_n)^2 - \omega_2^2]$ and $D_3 = 2\omega_3/[(i\nu_n)^2 - \omega_3^2]$.

In the actual calculations, we set $n = 1.5$ and the energy unit t is taken as $t = |(dd\sigma)|$. Note that we set $(dd\sigma) = -t$. For the sum on the imaginary axis, we use 131,072 Matsubara frequencies. As for the phonon energy, we set $\omega_2/t = \omega_3/t = 0.2$. We define the non-dimensional electron-phonon coupling constants as $\lambda_2 = 2g_2^2/(t\omega_2)$ and $\lambda_3 = 2g_3^2/(t\omega_3)$, which are set as $\lambda_2 = \lambda_3 = 0.8$.

In Fig. 1, we show the change of the Fermi surfaces, when we control the Slater-Koster integral $(dd\delta)/t$ from -2.0 to 2.0 for $(dd\sigma)/t = -1.0$. In Fig. 2, we show T_c/t vs. $(dd\delta)/t$. In the region of negative $(dd\sigma)$, we observe the overall tendency of the increase of T_c with the increase of $(dd\delta)/t$ from -2.0 to 0.0, except for the cusps at $(dd\delta)/t = -1.5$ and -0.7 due to the van Hove singularities. When we increase $(dd\delta)$ from zero, T_c is monotonically increased for $0 \le (dd\delta)/t \lesssim 0.2$. For $0.2 \lesssim (dd\delta)/t \lesssim 0.6$, there appears the single Fermi surface and T_c is totally low, since the density of states is suppressed in this region. However, when we increase $(dd\delta)$, T_c is rapidly increased. Around at $(dd\delta)/t = 0.6$, there occurs a new Fermi surface and the Fermi-surface topology is abruptly changed again, leading to the van Hove singularity. For $0.6 \lesssim (dd\delta)/t \lesssim 1.6$, T_c depends on the values of $(dd\delta)$, but we observe that the magnitude of T_c is kept high as $T_c/t = 0.005 \sim 0.01$, even though the Fermi-surface topology is changed in this region. Note that for $1.6 \lesssim (dd\delta)/t \le 2.0$, T_c is totally low and it is difficult to obtain T_c with enough precision in this region, since T_c approaches the lower limit which we can safely calculate.

The enhancement of T_c in the case of the plural numbers of the Fermi surfaces is explained by the enhancement of the pair-hopping attraction between Cooper pairs on different Fermi surfaces due to Jahn-Teller phonons [2]. This pair-hopping attraction does not work for the case of the single Fermi surface. Thus, T_c in the case of the plural numbers of the Fermi surfaces is enhanced in comparison with the case of single Fermi surfce. This enhancement mechanism still works even for the case of small-size pocket-like Fermi surfaces.

References

[1] Y. Shiba and T. Hotta: J. Phys.: Conf. Ser. **428** (2013) 012038.

[2] T. Hotta: J. Phys. Soc. Jpn. **79** (2010) 023709.

Phase formation and dynamics in correlated cold atom systems

NORIO KAWAKAMI
Department of Physics, Kyoto University, Kyoto 606-8502, Japan

In this decade, cold atom systems have attracted much attention as a new field, because of recent rapid progress in cooling and manipulation techniques [1]. The progress in these techniques has enabled experimentalists to cool confined atomic gases to nano-Kelvin temperatures, to make a lattice potential by using interfering laser beams, and also to modify strength and sign of interaction between cold atoms by Feshbach resonance. Further, these system parameters can be adapted in real time or instantaneously, so even the dynamics of cold atom systems is also enthusiastically studied. Therefore cold atom systems are expected to be quantum simulators of model Hamiltonians developed in the field of condensed matter physics.

One of the main issues in our research project is to study non-equilibrium dynamics of cold atom systems. We focus on drag dynamics of a trapped fermion cluster in a fermion cloud, from interest in non-equilibrium dynamics when the system parameters gradually change in real time. These systems are different from quantum quench systems in which the system parameters suddenly change and are fixed after that sudden change.

In this study we simulate the drag dynamics in the following system. Initially a cluster of n fermions is trapped by a harmonic potential within a cloud of the other type of free fermions, where the average fermion density of the cloud is D. The fermion cluster is trapped by a harmonic trap potential, and the interaction exists between two fermions of the different types. Then we suddenly move the trap potential and the cluster by a constant speed for the cluster to push the cloud.

We simulate this dynamics by using time-dependent density matrix renormalization group [2], and calculate the energy of the system. As a result, the moving trap increases the total energy of the system as a linear function of the time approximately. We evaluate the energy increase per unit time P from the energy-time plot.

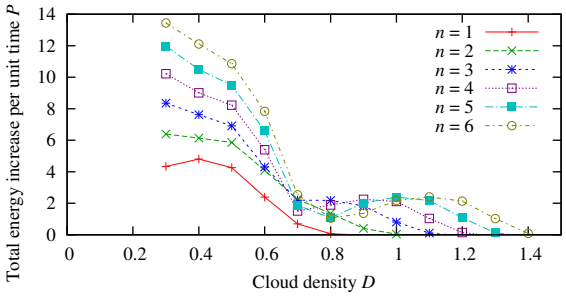

Figure 1: Energy increase per unit time P.

Figure 1 shows how P depends on n and D. In the $n = 1$ case, P has a single peak, but in the $n > 2$ case, P has double peaks. This double-peak structure is explained by our concise model, which includes quantum many-body effects. Our model suggests that the second peak is due to the dynamical collective modes in which momentum is properly distributed [3].

References

[1] D. Jaksch and P. Zoller, Ann. Phys. **315**, 52 (2005).

[2] S. R. White and A. E. Feiguin, Phys. Rev. Lett. **93**, 076401 (2004).

[3] J. Ozaki, M. Tezuka, N. Kawakami, to be published.

Analysis of Topological Phases in Strongly Correlated Systems

NORIO KAWAKAMI
Department of Physics, Kyoto University, Kyoto 606-8502, Japan

Recently, the topological band insulator (TBI) has attracted much interest as a new class of quantum phases, where the spin-orbit coupling plays an essential role. One of the current major issues is the influence of strong correlation effects upon the topological phase because electron correlations are expected to create new topological phases. This issue has further been stimulated by theoretical proposals in d- and f- electron systems [1].

One of the main issues in our research is to study the spatial dependence of electron correlations in these topological phases to clarify the edge state. In this study, we consider a generalized Bernevig-Hughes-Zhang model [2] having electron correlations with the variational Monte Carlo (VMC) method. In order to study how interactions affect the edge states and bulk states respectively, we introduce spatially-dependent variational parameters (Fig. 1).

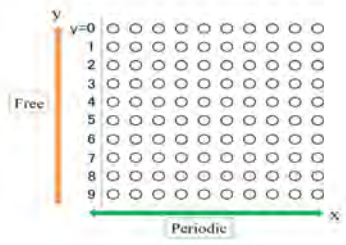

Figure 1: Periodic (free) boundary condition in the x (y) directions. $y = 0$ and $y = 9$ correspond to the boundary in this system.

To perform the large-scale numerical calculation, we have fully made use of the supercomputer resource at ISSP. Namely, we have optimized many spatially-dependent variational parameters efficiently, where we have performed large-scale MPI parallel computing.

Figure 2 shows average electron numbers at each y as functions of the interaction strength U. This result clearly evidences a first-order Mott transition, which is accompanied by a hysteresis. This result also shows that the average electron number at the edge sites ($y = 0$) decreases more rapidly than in the bulk because the coordination number at the edge sites is smaller. In this calculation, however, phase transitions simultaneously occur in the entire system and we cannot find the novel intermediate phase which is expected in some previous works.

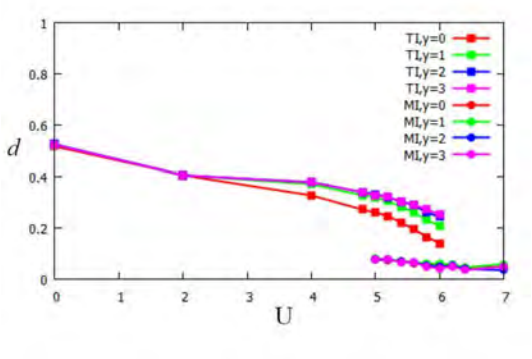

Figure 2: (Color Online). Average electron numbers at each y as functions of interaction strength U. The solid line with square (circles) represents the topological (Mott insulating) state.

We have also calculated the correlation functions to discuss the topological properties of this system. These will be reported elsewhere.

References

[1] T. Yoshida *et al.*, Phys. Rev. B **87**, 165109 (2013).

[2] B. A. Bernevig, T. L. Hughes and S. C. Zhang, Science **314**, 1757 (2006).

Ab initio calculations for iron-based superconductors FeTe and FeSe

Takahiro MISAWA

Department of Applied Physics, University of Tokyo,
7-3-1 Hongo, Bunkyo-ku, Tokyo 113-8656, Japan

Iron-based superconductors have diverse magnetic properties, although most of them have essentially the same band structures. For example, LaFeAsO (called 1111-type) shows the stripe antiferromagnetic (AFS) phase and its magnetic ordered moment is about $0.8\mu_{\rm B}$. The AFS phase is stable not only in the 1111-type compounds but also in the 122-type such as $BaFe_2As_2$. In contrast to this, FeTe (called 11-type) shows bicollinear antiferromagnetic state (AFB) and its ordered moment is about $2.0\mu_B$, while another 11-type compound FeSe does not show any magnetism but superconductivity appears below 10 K. Our previous studies show that this magnetic diversity can not be explained by the band structure alone and it is necessary to consider effects of electronic correlations [1,2].

To study the electronic correlation effects on the magnetism in iron-based superconductors, we employ *ab initio* downfolding scheme (for a review, see [3]). In this scheme, we first obtain the global band structures based on the density functional theory. From the band structures, we derive the low-energy effective models by using constrained random phase approximation. However, it is pointed out that double counting of the electron correlation between the low-energy states exists, and the effects of them are essential especially in the non-degenerate multi-band materials such as the iron-based superconductors [4]. To overcome this problem, constrained self-energy method is proposed, which can eliminate double counting of the electron correlations. In this method, the exchange-correlation energy in the conventional downfolding replaced with the self-energy corrections coming from the eliminated high-energy degrees of freedom as well as from the frequency-dependent part of the partially screened interactions.

In this study, we solve the low-energy effective models for FeTe and FeSe [5]. As a result, we find that the AFB state becomes the ground state in FeTe, while the AFS phase is the ground state in the previous effective model [6]. Moreover, we find that FeSe shows peculiar magnetic degeneracy, i.e., four different magnetic orders including AFS and AFB are energetically degenerate, while the AFS phase is also singled out in the previous model. This degeneracy may explain the absence of magnetic order and superconductivity observed in FeSe.

References

[1] T. Misawa, K. Nakamura, and M. Imada: J. Phys. Soc. Jpn. **80** (2011) 023704.

[2] T. Misawa, K. Nakamura, and M. Imada: Phys. Rev. Lett. **108** (2012) 177007.

[3] T. Miyake and M. Imada: J. Phys. Soc. Jpn. **79** (2010) 112001.

[4] H. Hirayama, T. Miyake, and M. Imada: Phys. Rev. B **87** (2013) 195144.

[5] H. Hirayama, T. Misawa, T. Miyake, and M. Imada: in preparation.

[6] T. Miyake, K. Nakamura, R. Arita, and M. Imada: J. Phys. Soc. Jpn. **79** (2010) 044705.

Effect of fluctuation near the ordered state in strongly correlated electron systems

Tetsuya MUTOU
Interdisciplinary Faculty of Science and Engineering, Shimane University
1060 Nishikawatsu-cho, Matsue, Shimane 690-8584

We studied some theoretical models of strongly correlated electron systems by numerical approach based on the many-body perturbation theory. To solve self-consistent equations in a three- or four-dimensional momentum-energy space, we carried out large-scale numerical calculations mainly on System A of the SCC-ISSP. In practical calculations, we applied simple program parallelizations to numerical integrals in the self-consistent equations.

With applying the fluctuation-exchange approximation to the single-band Hubbard model with realistic tight-binding parameters, we investigated the spin fluctuation effect in spin excitation spectra observed by neutron scattering experiments on electron-doped high-transition-temperature (high-T_c) superconductors [1]. In this study, we showed that the magnetic response of electron-doped high-T_c superconductors can be explained with the conventional Fermi-liquid approach.

The self-consistent second-order perturbation theory (SCSOPT) was applied to the multi-band Hubbard model corresponding to the electron system in bcc iron [2]. It was found that the spin stiffness constant is in good agreement with other theoretical results and it is smaller than the experimental value.

To investigate dynamical spin and density response functions in correlated fermion systems corresponding to two-dimensional (2D) liquid ^{3}He, the SCSOPT was also applied to the Hubbard model with repulsive interactions between fermions on up to fourth-neighbor sites [3]. It was pointed out that it is necessary to treat the large damping effect properly in explaining the propagating mode found in 2D liquid ^{3}He.

We investigated quasiparticle excitations in the periodic Anderson model which is one of models of the heavy Fermion systems by the dynamical mean-field theory with the iterated perturbation theory. We compared the renormalized Fermi energy of the quasiparticle with the effective hybridization energy, and investigated the quasiparticle-formation condition.

References

[1] T. Mutou and D. S. Hirashima: J. Phys. Soc. Jpn. **82** (2013) 094703.

[2] M. Nishishita, D. S. Hirashima, and S. Pandey: J. Phys. Soc. Jpn. **82** (2013) 114705.

[3] A. Kotani and D. S. Hirashima: Phys. Rev. B **88** (2013) 014529.

Numerical study of various phases and non-equilibrium phase transitions in correlated electron systems

Hideo AOKI
Department of Physics, University of Tokyo
Hongo, Tokyo 113-0033

Supersolid phase in electron-phonon systems[1, 2]

Competition and coexistence of various ordered phases are central issues of strongly correlated electron systems. Particularly interesting is the case where the diagonal and off-diagonal long-range order coexist. A primary example is the supersolid (SS) phase, in which superconductivity (SC) and charge order (CO) emerge simultaneously. Supersolid phases have long been pursued both theoretically and experimentally.

We have examined the existence of a supersolid phase in electron-phonon systems, in which a coexistence of e.g. s-wave SC and CO is known to occur in $Ba(Bi,Pb)O_3$ and $(Ba,K)BiO_3$. To this end, we take the Holstein model, one of the simplest and representative models for electron-phonon systems, and solve its ordered phases with the dynamical mean-field theory (DMFT). For the impurity solver of DMFT, we use the numerically exact continuous-time quantum Monte Carlo method, which has been extended so that one can treat SC, CO, and antiferromagnetic (AF) phases without bias[1, 2]. Obtained phase diagram for the intermediate electron-phonon coupling in the BCS-BEC crossover regime is shown in Fig. 1. One can see that SS phase appears between CO and SC phases, where the SS is accompanied by a quantum critical point (QCP) at zero temperature. We have checked that SS phase is indeed stable against phase separation. The transition from SC to SS is continuous with diverging charge fluctuations accompanied by a kink in the superfluid density.

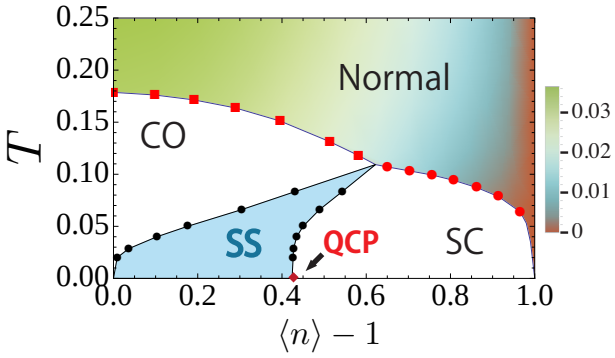

Figure 1: DMFT phase diagram of the Holstein model at the intermediate coupling regime [1]. The colour code in the normal phase represents the dc conductivity.

Nonequilibrium dynamical mean-field theory and its cluster extension[3, 4]

Nonequilibrium dynamical mean-field theory (DMFT) is a well-established approach to simulate nonequilibrium states of correlated many-body systems. It maps the original lattice model to an effective impurity embedded in the self-consistently determined mean-field bath. The essential approximation is to identify the local impurity self-energy with the lattice self-energy, which limits the range of applicability of the nonequilibrium

DMFT. The method has been applied to various systems, and provided fruitful insights for nonequilibrium systems. In view of the recent progress, we have written a review article on the nonequilibrium DMFT and its applications[3].

The local approximation for the self-energy may break down in low dimensional systems, where spatially nonlocal fluctuations play an essential role. To overcome this, we have proposed the nonequilibrium dynamical cluster approximation (DCA) [4], in which the lattice model is mapped to a multi-site cluster rather than a single impurity. As a result, one can take account of short-range correlations within the cluster size. We have applied it to the one- and two-dimensional Hubbard models. In Fig. 2, we plot the time evolution of the double occupancy and the jump of the momentum distribution at Fermi energy after an interaction quench at $t = 0$. We find characteristic momentum-dependent relaxations, which is attributed to the effect of nonlocal correlations.

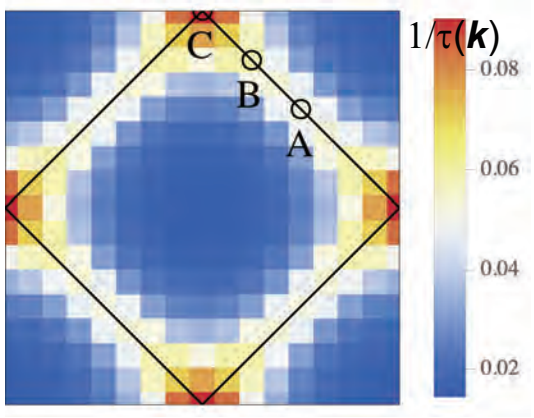

Figure 2: Colour-coded plot of the momentum-dependent quasiparticle lifetime $\tau(k)$ for an interaction quench $U/J = 0 \rightarrow 2$ at $T = 0$. Solid lines indicate the noninteracting Fermi surface.[4]

References

[1] Y. Murakami, P. Werner, N. Tsuji, and H. Aoki: Supersolid phase accompanied by a quantum critical point in the intermediated coupling regime of the Holstein model, arXiv:1402.6456.

[2] Y. Murakami, P. Werner, N. Tsuji, and H. Aoki: Ordered phases in the Holstein-Hubbard model: Interplay of strong Coulomb interaction and electron-phonon coupling, Phys. Rev. B **88**, 125126 (2013).

[3] H. Aoki, N. Tsuji, M. Eckstein, M. Kollar, T. Oka, and P. Werner: Nonequilibrium dynamical mean-field theory and its applications, to be published in Rev. Mod. Phys. (arXiv:1310.5329).

[4] N. Tsuji, P. Barmettler, H. Aoki, and P. Werner: Nonequilibrium dynamical cluster theory, arXiv:1307.5946.

Numerical Studies on Topological and Spin Liquid Phases of Iridium Oxides

Youhei YAMAJI
Department of Applied Physics, University of Tokyo
Hongo 7-3-1, Bunkyo-ku, Tokyo 113-8656

Cooperation and competition between strong electron correlations and spin-orbit couplings have recently attracted much attention. Iridium oxides offer the playgrounds and indeed exhibit intriguing phenomena. Especially, theoretical predictions on realization of novel quantum phases are interesting: The novel phases are condensed-matter realization of Weyl fermions predicted in magnetic phases of pyrochlore iridates $R_2Ir_2O_7$ (R: rare-earth elements) and a quantum spin liquid state with Majorana excitations in honeycomb iridates A_2IrO_3 (A=Na, Li).

The Weyl electrons in the bulk are shown to form metallic surface states called *Fermi arcs*, and to exhibit anomalous transports due to *chiral anomalies*, which have triggered intensive studies on the emergence of the Weyl electrons. However, the Weyl electrons are easily annihilated in pairs. The experimental observation requires fine tunings of the materials.

The spin liquid ground state proven by A. Kitaev for an exactly solvable model, now called Kitaev model, has also inspired extensive studies on A_2IrO_3 as a model system to realize the Kitaev's spin liquid. However, Na_2IrO_3 does not show spin liquid properties experimentally but exhibits a zigzag type magnetic order. A mechanism that stabilizes the zigzag magnetic order and a recipe to realize the Kitaev's spin liquid phase have remained controversial yet.

We revealed that magnetic domain walls in $R_2Ir_2O_7$ host metallic domain-wall states with Fermi surfaces, instead of arcs, even after pair-annihilatin of the Weyl electrons [1]. By using a fully unrestricted Hartree-Fock approximation for a Hubbard-type model of $J_{\rm eff} = 1/2$ states with large supercells at the system B, we show that domain walls perpendicular to $(01\bar{1})$, (100), and (111) directions host metallic domain-wall states. The insertion of the magnetic domain walls induces uniform magnetization. The uniform magnetization enables us to control the metallic domain-wall states with magnetic fields and explains weak ferromagnetism universally observed in $R_2Ir_2O_7$.

We also derived an *ab initio* effective spin model of Na_2IrO_3 [2], which has dominant Kitaev-type couplings together with newly-introduced anisotropy originating from the trigonal distortion. By using Arnoldi methods and thermal pure quantum states [3] at the system B, we show that the magnetic orders, specific heat, and magnetic susceptibilities of the effective spin model are indeed consistent with experiments. We also show how to approach spin liquids.

References

[1] Y. Yamaji and M. Imada: Phys. Rev. X, in press; arXiv:1306.2022.

[2] Y. Yamaji, Y. Nomura, M. Kurita, R. Arita, and M. Imada: arXiv:1402.1030.

[3] S. Sugiura and A. Shimizu: Phys. Rev. Lett. **108** (2012) 240401.

Electronic state calculations of quantum mechanical order appearing in metal compounds

Koichi KUSAKABE
Graduate School of Engineering Science, Osaka University
1-3 Machikaneyama, Toyonaka, Osaka 560-8531

1. Introduction

To derive unified representation of the strongly correlated electron systems (SCES), we need to utilize consistent determination of a basis for expansion of the Hilbert space, keeping description of the quantum fluctuation effects appearing as correlated many-body state vectors and many-body Green's functions. The multi-reference density functional theory[1, 2] gives an answer. For the real applications, we need to set up a good basis. In this study, we mainly focused on creation of a proper basis and estimation of scattering amplitudes appearing for each specific material system.

2. Estimation of electronic parameters and prediction of novel cuprates

A starting expression of the multi-layered cuprate superconductors may be taken as the DFT-GGA description of atomic structures. Actually, we found good convergence in the atomic structure around the experimentally observed structures.[3] We rely on the spin fluctuation mechanism of superconductivity for a judgment of an optimally doped cuprate. Recent confirmation of the correlation between the transition temperature and the Fermi surface shape[4] suggests that, when $3d_{3z^2-r^2}$ orbitals do not have notable contribution at the Fermi level, keeping the energy separation ΔE from $3d_{3z^2-r^2}$ to $3d_{x^2-y^2}$ large around 2eV, then the better Fermi surface nesting, the higher transition temperature appears.

To certify our procedure, we first confirmed that 1) we have small hole-doping dependence of the electronic structure parameters, *i.e.* ΔE and the Fermi surface shape controlling factor $r_{x^2-y^2}$, and 2) these parameters are almost same with little systematic change against the layer number of CuO_2 planes in the unit cell. Following the rule for the orbital distillation effect[6], we try to search for materials which show better sets of $(\Delta E, r_{x^2y^2})$.

We have chosen Hg1223 ($T_c \geq$ 135K) and Tl1223 ($T_c \geq$ 110K) for this optimization. Our analysis suggests that $TlR_2A_2Cu_3O_9$ with R=Li, Y, and A=Li, Na, K, Rb, Cs may appear as stable crystal structures. Among these candidates, we found better conditions on the above parameters for (R, A)=(Y, Li), (Y, Na), and (Y, Rb).[3, 5] When we substitute Cd for Hg in $HgBa_2Ca_2Cu_3O_8$, we have small $r_{x^2-y^2}$, keeping ΔE around 2eV, which is a good condition for the high T_c.

3. Doping mechanism of α-pyridine-TiNCl

The superconductivity in α-MNX compounds attracts interests because of their special two-dimensional electronic structures. Experimentally, origin of the electron carrier was not clarified for pyridine-TiNCl. We have proposed that reduction of pyridine by water molecules could be the solution. We have obtained the electronic structure of pyridinium-ion-doped pyridine-TiNCl. (Fig. 1) The conduction band is doped by pyridinium ion. The

conformation of pyridine layer is affected by the doping, which is though to be origin of change in inter-layer electronic scattering processes. We expect that this non-stoichiometry condition would mediate pair-hopping processes.

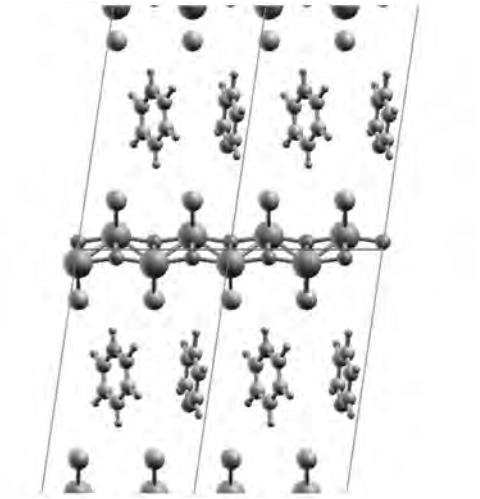

Figure 1: Optimized crystal structures of pyridinium-doped py-TiNCl.

4. Hydrogenated vacancies of graphene

In a recent study on argon sputtering and hydrogenation treatment of graphene, Ziatdinov *et al.* have succeeded in fabrication of various hydrogenated graphene vacancies.[7] They called stable structures V111 for the vacancy with three hydrogen atoms and V211 for the vacancy with four hydrogen atoms. The electronic structure shows a non-bonding localized state around V111, while V211 gives a gap at the Dirac point.

Utilizing the Löwdin charge analysis with the density of states, we concluded that the Fermi level is kept at the Dirac point for charge neutral hydrogenated graphene vacancies. This result suggests existence of a localized spin at V111. In addition, the experimental finding of bias induced carrier doping of graphene device structure suggests a possible Kondo state for V111.

Acknowledgement

The author (K.K.) is grateful to Prof. I. Maruyama, Mr. K. Yamada, Mr. S. Miyao, Mr. S. Gagus Ketut, Mr. Keisuke Iwatani, and Mr. Naoki Morishita for their collaboration. K. K. thanks fruitful collaboration in the study of hydrogenated graphene with Prof. T. Enoki, Prof. T. Mori, Prof. M. Kiguchi, Prof. K. Takai, Prof. S. Fujii, Mr. M. Ziatdinov, and Mr. Y. Kudo. K.K. is grateful to Prof. K. Kuroki, and H. Sakakibara for their collaboration in the study of cuprate superconductors. This work was partly supported by KAKENHI (No. 23540408), and the golbal COE program from MEXT.

References

[1] K. Kusakabe, *et al.*: J. Phys. Condens. Matter **19** (2007) 445009.

[2] K. Kusakabe and I. Maruyam: J. Phys. A: Math. Theor. **44** (2011) 135305.

[3] S. Miyao, *et al.*: arXiv:1304.5043.

[4] H. Sakakibara, *et al.*: arXiv:1403.2497.

[5] S. Miyao, *et al.*: J. Phys. Soc. Jpn. Suppl. **83** (2014) in press.

[6] H. Sakakibara, *et al.*: Phys. Rev. Lett. **105** (2010) 057003 .

[7] M. Ziatodinov, *et al.*: Phys. Rev. B **89** (2014) 155405.

Electronic properties of multi-orbital electronic system with strong spin-orbit coupling

Toshihiro SATO
Computational Condensed Matter Physics Laboratory, RIKEN
Wako, Saitama 351-0198, Japan

The transition-metal oxides have been studied as typical materials of strongly correlated electronic systems. Recent experimental studies have reported interesting behaviors of $5d$ transition-metal Ir oxides, for example Sr_2IrO_4. In these materials, there exists a strong spin-orbit coupling (SOC) with an electron correlation and the SOC splits the t_{2g} bands in the crystal field into the effective local angular momentum $J_{\rm eff}$=1/2 doublet and $J_{\rm eff}$=3/2 quartet bands. In Sr_2IrO_4 with totally five electrons, $J_{\rm eff}$=1/2 antiferromagnetic (AF) insulator has been observed against the expectation from $3d$ and $4d$ transition-metal Ir materials of the similar layered perovskite structure [1, 2, 3], and theoretical understanding in the experimental results has been successful by several numerical methods [1, 4, 5, 6, 7]. However, theoretical understanding of multi-orbital systems with the electron correlation and the SOC systematically is still controversial.

We study electronic and magnetic properties of the three-orbital Hubbard model with the full Hund' rule coupling and the SOC terms at five electrons filling,

$$
\begin{aligned}
H &= \sum_{\langle i,j\rangle,\gamma,\sigma} t^{\gamma} c^{\gamma\dagger}_{i\sigma} c^{\gamma}_{j\sigma} - \sum_{i,\gamma,\sigma} \mu^{\gamma} n^{\gamma}_{i\sigma}, \\
&+ U \sum_{i,\gamma} n^{\gamma}_{i\uparrow} n^{\gamma}_{i\downarrow} + \frac{U'-J}{2} \sum_{i,\gamma\neq\delta,\sigma} n^{\gamma}_{i\sigma} n^{\delta}_{i\sigma} \\
&+ \frac{U'}{2} \sum_{i,\gamma\neq\delta,\sigma} n^{\gamma}_{i\sigma} n^{\delta}_{i\bar{\sigma}} - J \sum_{i,\gamma\neq\delta} c^{\gamma\dagger}_{i\uparrow} c^{\gamma}_{i\downarrow} c^{\delta\dagger}_{i\downarrow} c^{\delta\dagger}_{i\uparrow} \\
&+ J' \sum_{i,\gamma\neq\delta} c^{\gamma\dagger}_{i\uparrow} c^{\gamma\dagger}_{i\downarrow} c^{\delta}_{i\downarrow} c^{\delta}_{i\uparrow} \\
&+ \lambda \sum_{1,\gamma,\delta,\sigma,\sigma'} \langle\gamma|\mathbf{L}_i|\delta\rangle \cdot \langle\sigma|\mathbf{S}_i|\sigma'\rangle c^{\gamma\dagger}_{i\sigma} c^{\delta}_{i\sigma'},
\end{aligned}
$$

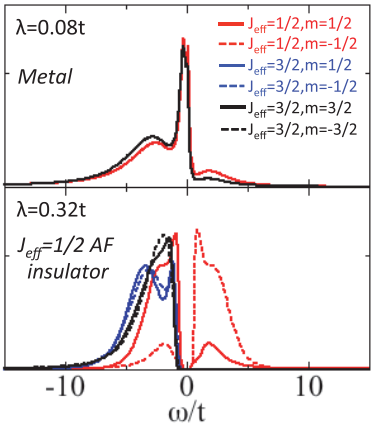

Figure 1: Density of states for two λ's at U=8t and T=0.06t .

where t^{γ} is the nearest-neighbor hopping amplitude with orbital γ=(yz, zx, xy) and μ^{γ} is the chemical potential. U (U') is the intra-orbital (inter-orbital) Coulomb interaction and J (J') is the Hund' s (pair-hopping) coupling, and we set U=U'+2J and J=J'=0.15U. λ is the SOC and $\mathbf{L}_i$ ($\mathbf{S}_i$) is the orbital (spin) angular momentum operator at site i. $c^{\gamma\dagger}_{i\sigma}$ ($c^{\gamma}_{i\sigma}$) is an electron creation (annihilation) operator with spin σ and orbital γ at site i and electron density operator is $n^{\gamma}_{i\sigma} = c^{\gamma\dagger}_{i\sigma} c^{\gamma}_{i\sigma}$. We use the dynamical mean field theory [8] employing a semielliptic bare density of states with the equal bandwidth (t^{γ}=t) for the three orbitals. We calculate the Green's functions inside the orbital by using the continuous-time quantum Monte Carlo solver based on the strong coupling expansion [9]. This numerical calculation was performed by the numerical computations with facilities at Supercomputer Center in ISSP, e.g., for λ=0.1t, U=8t, and T=0.06t, about 10^8 Monte Carlo sweeps

and averaging over 64 samples, and the self-consistency loop of the DMFT converges about 100 hours. We examine λ-dependence of electronic structure at U=8t and T=0.06t fixed, and then confirm the transition from metallic to insulating state with a magnetic order with varying λ as shown in Fig. 1. The insulating state shows $J_{\rm eff}$=1/2 AF insulator, indication of the half-filled $J_{\rm eff}$=1/2 and full-filled $J_{\rm eff}$=3/2 bands. Moreover, we find that excitonic insulating state by the electron-hole paring between $J_{\rm eff}$=1/2 and $J_{\rm eff}$=3/2 bands is induced by λ at larger U, in addition to the $J_{\rm eff}$=1/2 AF insulator.

This work was done in collaboration with Dr. T. Shirakawa and Dr. S. Yunoki.

References

[1] B. J. Kim *et al.*: Phys. Rev. Lett. **101**, (2008) 076402.

[2] B. J. Kim *et al.*: Science **323**, (2009) 1329.

[3] K. Ishii *et al.*: Phys. Rev. B **83** (2011) 115121.

[4] H. Watanabe *et al.*: Phys. Rev. Lett. **105**, (2010) 216410.

[5] T. Shirakawa *et al.*: J. Phys.:Conf. Ser. **273**, (2011) 012148.

[6] C. Martins *et al.*: Phys. Rev. Lett. **107**, (2011) 266404.

[7] R. Arita *et al.*: Phys. Rev. Lett. **108**, (2012) 086403.

[8] G. Kotliar *et al.*: Phys. Rev. Lett. **87**, (2001) 186401.

[9] P. Werner *et al.*: Phys. Rev. Lett. **97**, (2006) 076405.

Quantum Monte Carlo simulation and electronic state calculations in correlated electron systems

Takashi YANAGISAWA
Electronics and Photonics Research Institute
National Institute of Advanced Industrial Science and Technology (AIST)
AIST Central 2, 1-1-1 Umezono, Tsukuba 305-8568

The mechanisms of superconductivity in high-temperature superconductors have been extensively studied using various two-dimensional models of electronic interactions. The CuO_2 plane in cuprates plays an important role for the appearance of superconductivity. It is well known that the parent materials are a Mott insulator and the hole doping leads to superconductivity. In this report we present the results on the Mott transition of high temperature cuprates at half- lling. In the case of cuprates the insulating state is regarded as a charge-transfer insulator, We propose a wave function of Mott state on the basis of an improved Gutzwiller function. To use computers more efficiently, we performed parallel computing with 64 or 128 cores.

The three-band model that explicitly includes Oxygen p orbitals contains the parameters U_d, U_p, t_{dp}, t_{pp}, ϵ_d and ϵ_p. U_d is the on-site Coulomb repulsion for d electrons and U_p is that for p electrons. t_{dp} is the transfer integral between adjacent Cu and O orbitals and t_{pp} is that between nearest p orbitals. The energy unit is given by t_{dp}.

The Gutzwiller wave function is given as $\psi_G = P_G\psi_0$, where P_G is the Gutzwiller projection operator given by $P_G = \prod_i[1 - (1-g)n_{di\uparrow}n_{di\downarrow}]$ with the variational parameter in the range from 0 to unity. P_G controls the on-site electron correlation on the copper site. ψ_0 is a one-particle wave function such as the Fermi sea or the Hartree-Fock state with spin density wave. ψ_0 contains the variational parameters $\tilde{t}_{dp}$, $\tilde{t}_{pp}$, $\tilde{\epsilon}_d$ and $\tilde{\epsilon}_p$: $\psi_0 = \psi_0(\tilde{t}_{dp}, \tilde{t}_{pp}, \tilde{\epsilon}_d, \tilde{\epsilon}_p)$. In the non-interacting case, $\tilde{t}_{dp}$ and $\tilde{t}_{pp}$ coincide with t_{dp} and t_{pp}, respectively. In this report, we consider the Gutzwiller function with an optimization operator:

$$\psi = \exp(\lambda K)\psi_G, \tag{1}$$

where K is the kinetic part of the total Hamiltonian H_{dp} and λ is a variational parameter. This type of wave function is an approximation to the wave function in quantum Monte Carlo method[1, 2, 3]. The computations were performed by using the variational Monte Carlo method.

The above wave function of course can be regarded as a wave function for the Mott state of the single-band Hubbard model. We rst show the results for the single-band Hubbard model. In Fig.1 we show the energy per site as a function of U. The Gutzwiller parameter g is shown in Fig.2 which indicates that g vanishes at a critical value U_c. The state with vanishing g would be an insulating state because of vanishingly small double occupancy. It is seen from Fig.1 that the energy changes the curvature near $U \sim U_c$. The energy is well approximated by a function of C/U with a constant C when U is large:

$$\frac{E}{N} \sim -C\frac{t^2}{U} \propto -CJ. \tag{2}$$

This means that the energy gain mainly comes from the exchange interaction which is of the order of $1/U$.

The gure 3 exhibits the ground state energy per site $E/N - \epsilon_d$ as a function of $\Delta_{dp} \equiv \epsilon_p - \epsilon_d$ for the d-p model. We can nd that the curvature of the energy, as a function of Δ_{dp}, is changed near $\Delta_{dp} \sim 2$. The energy is well

tted by $1/\Delta_{dp}$ shown by the dashed curve in Fig.3 when Δ_{dp} is greater than a critical value. This is because the most energy gain comes from the exchange interaction between nearest neighbor d and p electrons. This exchange interaction, denoted by J_K, is given by $J_K = t_{dp}^2(1/\Delta_{dp} + 1/(U_d - \Delta_{dp}))$. In the low carrier limit with large level di erence Δ_{dp}, the second term in the exchange coupling gives a negligible contribution. Thus, the effective exchange coupling J_K is approximated as $J_K = t_{dp}^2/\Delta_{dp}$. In the insulating state the energy gain is proportional to J_K,

$$\Delta E = \frac{E}{N} - \epsilon_d \simeq -C\frac{t_{dp}^2}{\Delta_{dp}} = -CJ_K, \qquad (3)$$

for a constant C. The critical value of Δ_{dp} is $(\Delta_{dp})_c \simeq 2t_{dp}$. When $t_{dp} \sim 1.5$eV, the charge-transfer gap is about 3eV.

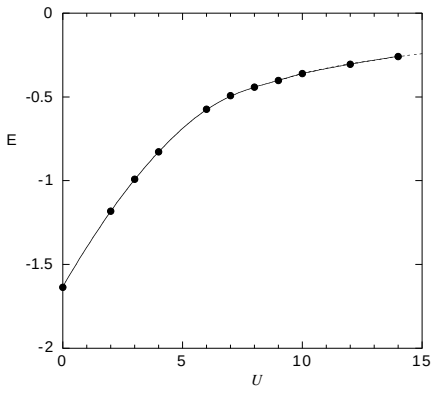

Figure 1: Ground state energy of the 2D Hubbard model as a function U at half- lling. The system size is 6×6.

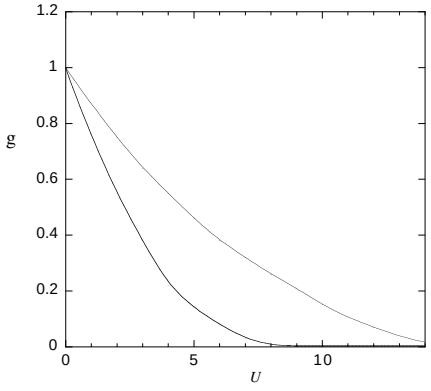

Figure 2: Gutzwiller parameter g as a function of U at half- lling. The parameter g almost vanishes at $U \sim 8$ showing a transition to an insulating state. The upper line is for $\lambda = 0$ (Gutzwiller function).

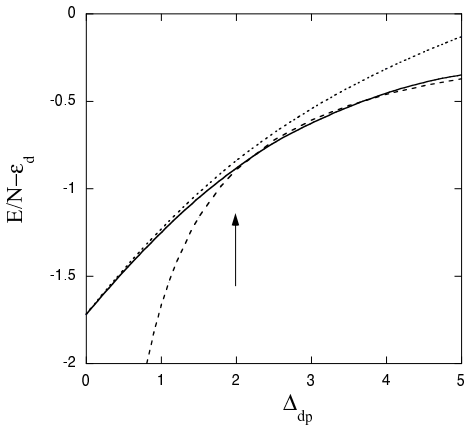

Figure 3: Ground state energy of the 2D d-p model as a function of Δ_{dp} for $t_{pp} = 0.4$ and $U_d = 8$ (in units of t_{dp}) in the half- lled case. The calculations were performed on 6×6 lattice. The arrow indicates a transition point, where the curvature is changed. The dotted curve is for the Gutzwiller function ($\lambda = 0$). The dashed curve indicates a curve given by a constant times $1/(\epsilon_p - \epsilon_d)$.

References

[1] T. Yanagisawa, Phys. Rev. B**75**, 224503 (2007) (arXiv: 0707.1929).

[2] T. Yanagisawa, New J. Phys. 15, 033012 (2013).

[3] T. Yanagisawa and M. Miyazaki, preprint (2014).

Dynamical Jahn-Teller Effect in Spin-Orbital Coupled System

Sumio ISHIHARA
Department of Physics, Tohoku University
Sendai 980-8578

No signs for long-range magnetic ordering down to the low temperatures, termed the quantum spin-liquid (QSL) state, are one of the fascinating states of matter in modern condensed matter physics. A number of efforts have been made to realize the QSL states theoretically and experimentally. A transition-metal oxide, $Ba_3CuSb_2O_9$ [1, 2], is a new candidate of the QSL state, in which S = 1/2 spins in Cu^{2+} ions are responsible for the magnetism. Almost isotropic g factors observed in ESR provide a possibility of no static long-range orbital orders and novel roles of orbital on the QSL.

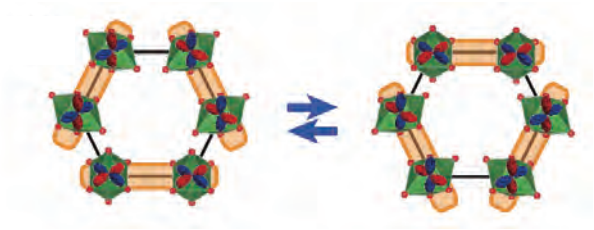

Figure 1: A schematic picture for the SORS. Shaded bonds represent the spin-singlet and parallel-orbital bonds.

We examine a possibility of the QSL state in a honeycomb-lattice spin-orbital (SO) system [3]. Beyond the previous theories for QSL in quantum magnets with the orbital degree of freedom, the present study focuses on the dynamical Jahn-Teller (DJT) effect, which brings about a quantum tunneling between stable orbital-lattice states. We suggest that a spin-orbital resonant state (SORS), where the two degrees of freedom are entangled with each other (see Fig. 1), is induced by the DJT effect.

First, we derive the low-energy electron-lattice model where the super-exchange interaction, the JT effect, and the lattice dynamics are taken into account, that is, $\mathcal{H} = \mathcal{H}_{\rm exch} + \mathcal{H}_{\rm JT}$. The Hamiltonian is analyzed by the exact-diagonalization method combined with the mean-field approximation, and the quantum Monte Carlo simulation with the mean-field approximation.

The phase diagram on a plane of the J_{DJT}-J_{SE} is shown in Fig. 2, where J_{DJT} and J_{SE} are amplitudes of the DJT effect and the super-exchange interaction, respectively. The spin-orbital resonant state appears in intermediate region of J_{DJT} and J_{SE}, that is, this quantum resonant state is realized by interplay of the two interactions. An obtained schematic picture for the spin-orbital resonant state is presented in Fig. 1 where the spin-singlet states and the parallel-orbital states occurs cooperatively.

To demonstrate the spin-orbital entanglement from the viewpoint of dynamics, we show, in Fig. 2, the dynamical spin-correlation function $K_s(\omega)$ and the dynamical orbital correlation function $K_\tau(\omega)$ calculated by using the Lanczos method in finite size clusters. Gapped spin excitations and low-lying orbital excitations are seen in the spin-orbital resonant state. In the resonant phase, in contrast to the orbital-ordered phase, an intensive or-

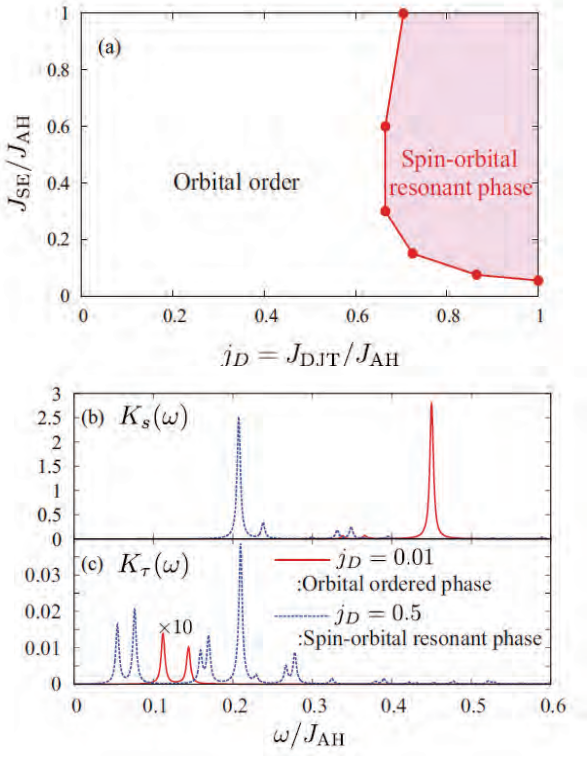

Figure 2: Upper: Phase diagram on the plane of J_{DJT}/J_{AH} and J_{SE}/J_{AH}. Lower: The dynamical spin-correlation function $K_s(\omega)$, and the dynamical orbital-correlation function $K_\tau(\omega)$ in the orbital ordered phase and in the SO resonant phase.

bital excitation is seen around the lowest spin-excitation energy.

The present theory provides a number of forceful predictions in $Ba_3CuSb_2O_9$. There will be a crossover frequency/magnetic field in ESR, corresponding to J_{DJT} and J_{SE}, where the anisotropy in the g factor is changed qualitatively. Dynamics of the orbital-lattice coupled vibronic excitation is expected to be observed directly by inelastic light/x-ray scattering spectra around 1$\sim$ 10 meV.

This work was supported by KAKENHI from MEXT and Tohoku University “ Evolution ” program. Parts of the numerical calculations are performed in the supercomputing systems in ISSP, the University of Tokyo.

References

[1] S. Nakatsuji, K. Kuga, K. Kimura, R. Satake, N. Katayama, E. Nishibori, H. Sawa, R. Ishii, M. Hagiwara, F. Bridges, T. U. Ito, W. Higemoto, Y. Karaki, M. Halim, A. A. Nugroho, J. A. Rodriguez-Rivera,M. A. Green, and C. Broholm, Science **336**, 559 (2012).

[2] Y. Ishiguro, K. Kimura, S. Nakatsuji, S. Tsutsui, A. Q. R. Baron, T. Kimura, and Y. Wakabayashi, Nat. Commun. **4**, 2022 (2013).

[3] J. Nasu and S. Ishihara, Phys. Rev. B **88**, 094408 (2013).

An Efficient Impurity Solver for Tomonaga-Luttinger Liquids

Kazumasa HATTORI

Institute for Solid State Physics,

University of Tokyo, Kashiwa-no-ha, Kashiwa, Chiba 277-8581

Continuous-time quantum Monte Carlo (CTQMC) methods have been developed and widely used for solving quantum impurity problems in strongly correlated electron systems in recent years [1]. They are numerically exact methods and used for not only fermionic systems but also bosonic ones including fermion-boson mixtures.

In this study, we have developed a CTQMC for bosonized Tomonaga-Luttinger (TL) liquids in one-dimensional systems. Technically, this is rather different from existing bosonic CTQMC, because of the dual (fermion/boson) nature of one-dimensional electron systems, which is highlighted in the existence of the Klein factors, various vertex operators relevant to interesting physical quantities, and ultraviolet cutoff (a) that is essentially infinity (i.e., continuous limit).

For a short summary of our results, we here show results for a back-scattering potential model in a spinless-fermionic system investigated by Kane and Fisher [2]. Figure 1 shows imaginary-time (τ) dependence of (left-moving) electron Green's function (G) calculated in the bosonization scheme in the CTQMC with several different values of a, the TL parameter g, and the inverse of temperature β. This clearly indicates that the asymptotic form of G is $\sim 1/\tau^{1/2g}$, which supports a prediction by Furusaki [3].

Since our method can be applicable to other models easily, we expect that various non-trivial physics in impurity problems in TL liquids will be clarified in future investigations.

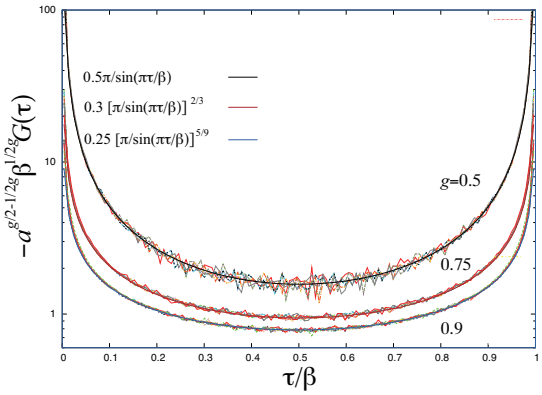

Fig. 1: G vs. τ for g = 0.9, 0.75, and 0.5, with three sets of cutoff a =1, 0.5, 0.25 and β = 200, 400, and 800. For large τ (~β/2), all the data are scaled into the functional form indicated in the figure.

References

[1] See for a review: E. Gull et al,: Rev. Mod. Phys. **83** (2011) 349.

[2] C. L. Kane and M. P. A. Fisher: Phys. Rev. Lett. **68**, (1992) 1220.

[3] A. Furusaki: Phys. Rev. B **56** (1997) 9352

Multiple enhancement mechanism of the dynamic spin-fluctuation in the iron based superconductors

Hayato ARAI, Yuki FUSEYA
University of Electro-Communications
1-5-1 182-0021 Chofugaoka, Chofu, Tokyo

Since the iron based superconductor LaFeAsO was found in 2008, many scientists have discussed about its mechanism of superconductivity. First, a mechanism of the phonon mediated superconductivity was proposed[1]. Then, a mechanism of the spin-fluctuation mediated superconductivity was proposed [2]. After that, a mechanism of the orbital fluctuation mediated superconductivity was proposed[3] in order to explain the impurity effect of iron based superconductors. However, we have not reached a consensus on the mechanism of the iron based superconductor yet. Our purpose is to clarify the mechanism of superconductivity of the iron pnictide on the basis of the spin-fluctuation mechanism. The reason why we focus on the spin-fluctuation mechanism is the fact that the superconducting phase locates next to the antiferromagnetic phase.

We adopted a multi-orbital Hubberd model in order to consider the complicated inter-orbital interactions of the iron pnictide. We constructed the five energy band model of LaFeAsO based on the first principle calculation and the most localized Wannier functions. We apply the FLuctuation EXchange (FLEX) approximation to this model. This calculation solves the multi-orbital Dyson equation self consistently and gives Green's functions that include the effect of interactions. T_c is calculated by solving the linearized Eliashberg equation with this Green's functions. We need to calculate the process using ISSP since we should vectorize the large matrix multiplication in order to reduce the calculation time. The accurate results we required need some self-consistent calculations with $32 \times 32 \times 1$ k-points, 5×2 orbitals and 4096 Matsubara frequency system size in system-B. We cannot consider the scale calculations without the ISSP system.

We have already known some results of the T_c measurement and the low-energy spin-fluctuation by the NMR experiment of $LaFeAs_{1-x}P_xO_{1-y}F_y$[4]. It is known that the P-doping distorts the crystal structure. The degree of this distortion can be parameterized by the Fe-As-Fe bond angle α. We calculated the orbital dependent dynamic spin-susceptivity and solved the linearized Eliashberg equation as a function of α.

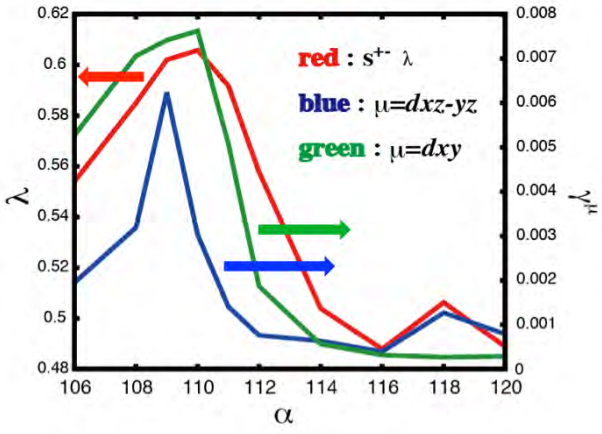

FIG. 1. Eigenvalue λ and low-energy spin-fluctuation γ versus Fe-As-Fe bond angle α. μ denotes the orbital.

The calculated results of the low-energy spin-fluctuations (γ^μ ; μ denotes the orbital

dependence) and the eigenvalue of the linearized Eliashberg equation (λ), which are shown in Fig 1. There is a clear correlation between λ and γ^{μ}. It is found that λ exhibits a double-peak structure : the peak of λ around 110° is due to the spin-fluctuation of both γ^{dxz-yz} and γ^{dxy} while the peak around 118° is due to that of only γ^{dxz-yz}. We conclude that the present theoretical results can give an interpretation of the experimental results that T_c exhibits the double peak structure as a fundtion of P-doping.

[1] L. Boeri, O. V. Dolgov, and A. A. Golubov, Phys. Rev. Lett. **101**, 026403 (2008).

[2] I. Mazin, D. J. Singh, M. D. Johannes, and M. H. Du, Phys. Rev. Lett. **101**, 057003 (2008).

[3] H. Kontani and S. Onari, Phys. Rev. Lett. **104**, 157001 (2010).

[4] H. Mukuda, *et al*, J. Phys. Soc. Jpn. **89**, 064511 (2014).

Development of Nonlocal Dynamical CPA and Numerical Study of Long-Range Magnetic Correlations

Yoshiro KAKEHASHI, M. Atiqur R. PATOARY, and Sumal CHANDRA
Department of Physics and Earth Sciences, Faculty of Science, University of the Ryukyus, 1 Senbaru, Nishihara, Okinawa, 903-0213, Japan

Development of the theory to describe nonlocal electron correlations is one of the central issues in condensed matter physics. Although the effective medium approaches such as the dynamical cluster approximation and the cluster dynamical mean field theory have been developed and can treat nonlocal correlations self-consistently, the range of nonlocal correlations are limited. In order to take into account the long-range inter-site correlations systematically, we developed the dynamical cluster CPA. The theory is an extension of the dynamical CPA [1] and takes into account the long-range nonlocal correlations by making use of the off-diagonal effective medium and the incremental cluster expansion.

The thermal averages of the physical quantities are obtained by solving the isothermal molecular-dynamics (MD) equations for the field variables $\{\xi_i\}$.

$$\dot{\xi}_i = \frac{1}{\mu_{\rm LM}} p_i, \tag{1}$$

$$\dot{p}_i = \frac{1}{2} U\Big(\langle m_i(\xi)\rangle - \xi_i\Big) - \eta_i\, p_i, \tag{2}$$

$$\dot{\eta}_i = \frac{1}{Q}\Big(\frac{p_i^2}{\mu_{\rm LM}} - k_{\rm B}T\Big). \tag{3}$$

Here U is the Coulomb energy parameter, p_i is the momentum being conjugate to the fictitious local moment variable ξ_i on site i, η_i is the friction variable on site i, $\mu_{\rm LM}(Q)$ is a mass for local moment (friction variable), and $m_i(\xi)$ is the average magnetic moment given by

$$m_i(\xi) = \frac{1}{\beta}\sum_{\sigma}\sigma \sum_{l=-\infty}^{\infty} \tilde{G}_{ii\sigma}(\xi, l), \tag{4}$$

$\tilde{G}_{ii\sigma}(\xi, l)$ being a Green function projected onto the static field variable $\{\xi_i\}$.

Figure 1 shows a numerical example of magnetization vs temperature curve for the single-band Hubbard model on the fcc lattice in the high-temperature approximation. Although the accuracy is not enough because of a small number of MD steps (typically 3000 steps), calculated $T_{\rm C}$ is about 0.085. It indicates that the Curie temperature is reduced by 50% by means of the long-range nonlocal correlations.

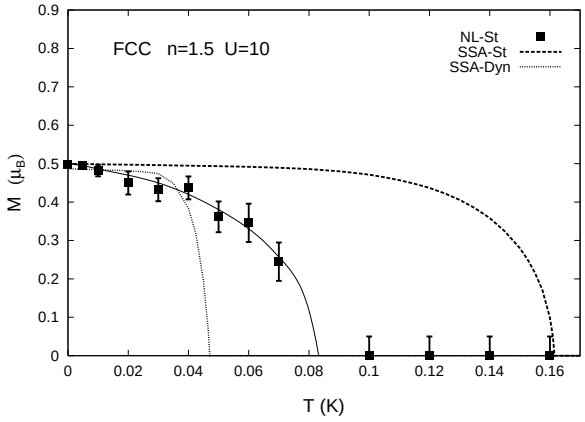

Figure 1: Calculated magnetization vs. temperature curves for the single-site static CPA (dashed-line), dynamical CPA (dotted curve), and the nonlocal dynamical CPA with static approximation (closed circles with error bars and thin line).

References

[1] Y. Kakehashi: Adv. Phys. **53**, (2004) 497; 'Modern Theory of Magnetism in Metals and Alloys' (Springer, Heidelberg, 2013).

Quantum Monte Carlo Approach to Odd-Frequency Superconductivity

Shintaro HOSHINO
Department of Basic Science, The University of Tokyo, Meguro, Tokyo 153-8902, Japan

Strongly correlated electron systems show a variety of intriguing phenomena including unconventional superconductivity. Especially we address the odd-frequency (OF) superconductivity, which is characterized by the pairing amplitude that is an odd function with respect to time. Such exotic pairing state is first proposed by Berezinskii for ^{3}He, and has been attracting attention as a candidate mechanism for unconventional superconductivities [1, 2].

The concrete realization of the OF superconductivity has been theoretically discussed in a variety of electron systems. One of possible realizations is proposed in the two-channel Kondo system by Emery and Kivelson using the impurity model [3]. In higher dimensions, the two-channel Kondo lattice (TCKL), where the periodically aligned localized spins couple to conduction electrons with two degenerate channels, has been investigated by using the dynamical mean-field theory (DMFT) [4]. However the divergent pairing susceptibility has not yet been found, and the existence of the OF superconductivity has remained unclear.

To clarify whether the OF superconductivity is realized in the TCKL, we have revisited this problem by using the DMFT. In this theory, the periodic system is mapped onto the effective impurity system, where one localized spin interacts with a bath of conduction electrons. We choose the continuous-time quantum Monte Carlo (CTQMC) method as the numerical impurity solver [5]. The algorithm we have used is based on the perturbation expansion of the partition function with respect to the interaction. The physical quantities are then evaluated as a Monte Carlo integration. In the present model, there is no sign problem fortunately. However, the calculation becomes heavy at low temperatures since we have to incorporate the contribution from higher-order perturbations. This difficulty can be reduced by the large-scale parallel calculation using the system B.

With use of the method illustrated above, we have successfully demonstrated the divergence of the OF pairing susceptibility [6]. Figure 1 shows the phase diagram of the TCKL obtained by the CTQMC, where the OF superconductivity is found at low temperatures.

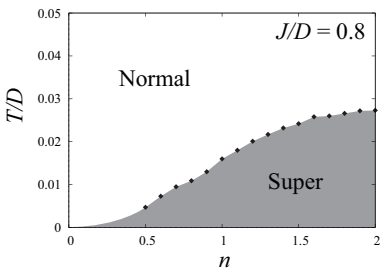

Figure 1: Phase Diagram of the TCKL. Here n, J, D and T are the filling of conduction electrons per site, interaction strength, half band width and temperature, respectively.

References

[1] V. L. Berezinskii: JETP Lett. **20** (1974) 287.

[2] Y. Tanaka, M. Sato, and N. Nagaosa: J. Phys. Soc. Jpn. **81** (2012) 011013.

[3] V. J. Emery and S. Kivelson: Phys. Rev. B **46** (1992) 10812.

[4] M. Jarrell, H. Pang, and D. L. Cox: Phys. Rev. Lett. **78** (1997) 1996.

[5] E. Gull *et al.*: Rev. Mod. Phys. **83** (2011) 349.

[6] S. Hoshino and Y. Kuramoto: Phys. Rev. Lett. **112** (2014) 167204.